This version is available at https://strathprints.strath.ac.uk/42840/

Induced magnetic moment of Eu^{3+} ions in GaN

V. Kachkanov[1], M. J. Wallace[2], G. van der Laan[1], S. S. Dhesi[1], S. A. Cavill[1], Y. Fujiwara[3] & K. P. O'Donnell[2]

[1]Diamond Light Source, Chilton, Didcot, Oxfordshire, United Kingdom, OX11 0DE, UK, [2]Department of Physics, University of Strathclyde, Glasgow, Scotland, United Kingdom, G4 0NG, Scotland, UK, [3]Division of Materials and Manufacturing Science, Graduate School of Engineering, Osaka University, 2-1 Yamadaoka, Suita, Osaka 565-0871, Japan.

Magnetic semiconductors with coupled magnetic and electronic properties are of high technological and fundamental importance. Rare-earth elements can be used to introduce magnetic moments associated with the uncompensated spin of 4f-electrons into the semiconductor hosts. The luminescence produced by rare-earth doped semiconductors also attracts considerable interest due to the possibility of electrical excitation of characteristic sharp emission lines from intra 4f-shell transitions. Recently, electroluminescence of Eu-doped GaN in current-injection mode was demonstrated in p-n junction diode structures grown by organometallic vapour phase epitaxy. Unlike most other trivalent rare-earth ions, Eu^{3+} ions possess no magnetic moment in the ground state. Here we report the detection of an induced magnetic moment of Eu^{3+} ions in GaN which is associated with the $^7F_2$ final state of $^5D_0 \rightarrow {}^7F_2$ optical transitions emitting at 622 nm. The prospect of controlling magnetic moments electrically or optically will lead to the development of novel magneto-optic devices.

G aN and related (In,Al,Ga)N alloys have become technologically important materials over the past fifteen years due to their unique physical properties, which include a wide direct bandgap, remarkable mechanical strength and high melting temperature. Commercial use of nitrides spans a broad field from optoelectronics to microwave technology. Besides being super-efficient light emitters on their own account, nitride semiconductors also prove to be promising hosts for visible- and infrared-emitting trivalent rare-earth (RE^{3+}) ions[1,2]. The luminescence of RE^{3+} ions is an attractive source of emission which is relatively independent of the ambient temperature and host material[3]. The use of semiconductors as hosts for RE ions has attracted much interest recently for the potential integration of RE emission with existing semiconductor devices. The discovery by Favennec et al.[4] that wide bandgap hosts reduce the temperature quenching of RE luminescence led to a widespread interest in doping of III-nitride semiconductors with RE^{3+} ions. More recently, attempts to exploit another property of the 4f-shell, namely the uncompensated spin of electrons, in order to produce dilute magnetic semiconductor, have been reported[5,6].

Doping GaN with Eu is particularly attractive for the realization of red light-emitting devices[7] due to problems related to the growth of InGaN with the moderately high InN fractions, required to produce intrinsic red emission from this alloy[8]. The first Eu-doped GaN electroluminescent devices, operating at a bias of $\sim$50 V, were reported by Heikenfeld et al.[9]. Recently, the first current-injection light emitting diode (LED), operating at voltages as low as 3 V, was realised by one of the present authors[10]. Stimulated emission from Eu-doped GaN has also been reported[11].

Interestingly, the observation of a ferromagnetic phase in Eu-doped GaN epilayers was first reported nearly a decade ago[12]. The presence of the ferromagnetism was attributed to the coexistence of magnetic Eu^{2+} species along with EuGaN since Eu^{3+} is non-magnetic. Hite et al.[13] reconfirmed the existence of a ferromagnetic response from Eu-doped GaN. However, no second phase formation was observed in the samples[13] and it was pointed out that no Eu phases are ferromagnetic at room temperature; the secondary phases considered include EuGa, EuGa$_2$, EuGa$_4$, Eu$_3$Ga$_8$, Eu$_5$Ga$_8$, metallic Eu, EuN, EuO, Eu$_3$O$_4$ and Eu$_2$O$_3$. On the other hand, two of the present authors recently reported the Zeeman splitting of emission lines at $\sim$622 nm assigned to the $^5D_0 \rightarrow {}^7F_2$ transition of Eu^{3+} centres in GaN with the magnetic field applied along the c-axis[14]. The observed Zeeman splittings, with g-factors $\sim$2, were suggested to be associated with the magnetic moment of the final $^7F_2$ state of the $^5D_0 \rightarrow {}^7F_2$ transition, since the $^7F_0$ ground state and $^5D_0$ excited state of Eu^{3+} ions do not have any associated magnetic moments.

In this work we report the detection of the induced magnetic moment associated with the $^7F_2$ state of Eu^{3+} ions which is involved in optical emission. We used X-ray magnetic circular dichroism (XMCD), which is the difference between the X-ray absorption spectra (XAS) for left- and right-circularly polarized X-rays. XMCD
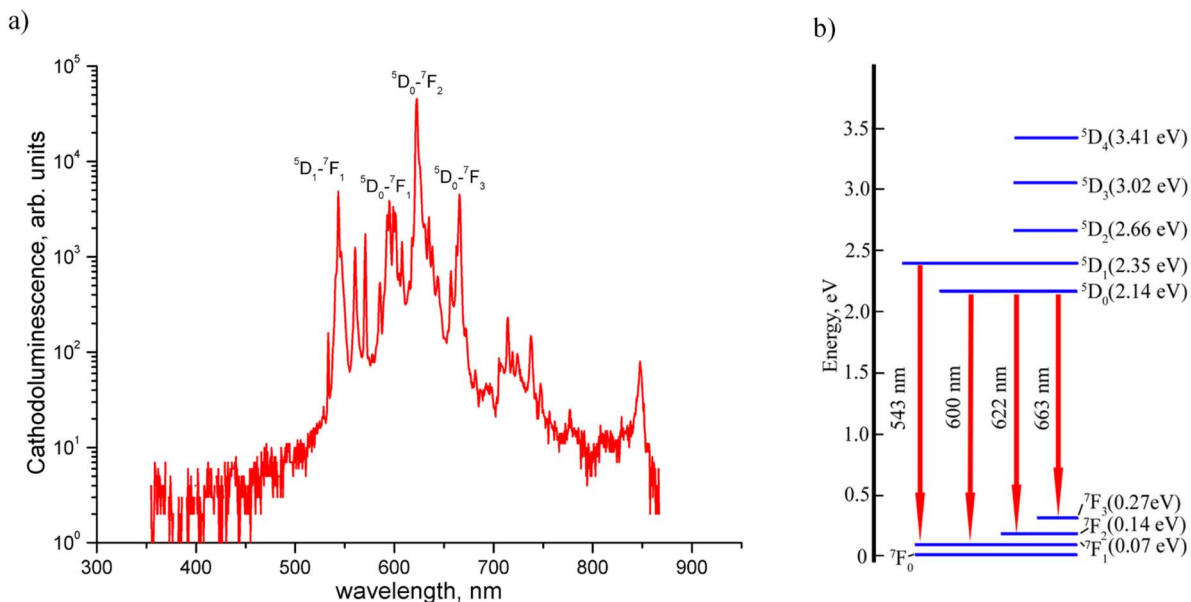
Figure 1 | Cathodoluminescence spectroscopy. (a) Room temperature CL spectrum obtained with an electron beam energy of 6 kV and beam current of 10 nA. The electron beam was defocused to a spot size of 10 μm. (b) Energy level diagram with emission lines due to intra-4*f* shell transitions for Eu³⁺ ions in GaN.

probes the magnetic moments of the states involved in the element-specific X-ray absorption process utilizing the helicity of the circularly polarized photons parallel and antiparallel to the sample magnetization direction[15]. To measure the induced magnetic moment of Eu³⁺ ions, the bright red Eu-related luminescence (with photon energy ~2 eV) emitted following X-ray excitation, referred to as X-ray excited optical luminescence (XEOL), was monitored with the X-ray energy scanned across the Eu M_4 (~1158 eV) and M_5 (~1128 eV) absorption edges ($3d_{3/2,5/2} \rightarrow 4f$ transitions). Conventional XMCD measurements were also taken, by detecting secondary X-ray fluorescence (XRF) and the drain current caused by Auger and secondary electrons, commonly referred to as total electron yield (TEY) detection.

Results

Sample structure and cathodoluminescence spectroscopy. The sample studied was GaN doped with Eu *in-situ* during growth by organometallic vapor phase epitaxy (OMVPE)[16]. The thickness of the doped layer was 400 nm. The concentration of Eu, estimated by Rutherford backscattering spectrometry (RBS), was 0.11 at%[17] corresponding to 9.6×10^{19} cm⁻³. Fig. 1 shows the cathodoluminescence (CL) spectrum of the sample at room temperature. Several emission lines are observed, identified as $^5D_1 \rightarrow ^7F_1$, $^5D_0 \rightarrow ^7F_1$, $^5D_0 \rightarrow ^7F_2$ and $^5D_0 \rightarrow ^7F_3$ intra-4*f* shell transitions at ~543 nm, 600 nm, 622 nm and 663 nm, respectively, according to the Dieke diagram[18,19]. Energy states for RE³⁺ ions are labelled following the Russell-Saunders scheme[3] as $^{2S+1}L_J$, in which S is the total spin angular momentum, L is the total orbital angular momentum and $J = L+S$ is the total angular momentum. The total momenta S and L are vectorial sums of individual electron spins and orbital moments, respectively. For energy levels with $J = 0$, the orbital moment compensates the spin moment, so that Eu³⁺ has no magnetic moment in the $^7F_0$ ground state. The 'hypersensitive' emission line at 622 nm is by far the brightest transition. Note that GaN band edge emission in the 350–400 nm spectral region is not observed: it is very much weaker than Eu³⁺ emission which dominates the entire CL spectrum of GaN:Eu.

X-ray magnetic circular dichroism. Fig. 2 shows the XMCD and corresponding XAS recorded by TEY and XEOL. Due to the

extremely low Eu concentration the XAS are dominated by the $L_{2,3}$ absorption from Ga atoms. The XMCD feature corresponding to the M_5 absorption peak due to the $3d_{5/2} \rightarrow 4f$ transition appears at 1128.3 eV and 1129.8 eV in TEY and XEOL, respectively. When the magnetic field is reversed the XMCD features in both TEY and XEOL reverse in sign at the same energy positions as expected, thereby confirming the reliability of the observation. Note that the difference in energy of the XMCD peaks for TEY and XEOL is 1.5 eV. The M_4 absorption peak corresponding to the $3d_{3/2} \rightarrow 4f$ transition is present in TEY at ~1157 eV and not resolved in XEOL. No XMCD features were observed using secondary XRF detection.

The experimentally observed difference in the XMCD peak positions for TEY and XEOL can be explained by taking into account the depth sensitivity and underlying physics of each detection method. TEY is a surface sensitive, where the signal probes the sample surface with an attenuation length of ~5 nm. X-ray photoelectron spectroscopy, with an even smaller probing depth, indicates that Eu³⁺ undergoes a valence-state transition into Eu²⁺ near the surface of GaN[20]. The presence of a 10 nm thick GaN cap in the sample should therefore reduce the bulk TEY signal by 86%; it is also possible that Eu ions diffuse through the GaN cap. In any case, the XMCD measured by TEY clearly indicates the presence of Eu²⁺ ions at the surface of GaN.

On the other hand, visible photons emitted by Eu³⁺ are collected from the entire depth of the epilayer. Since the visible luminescence of the sample is dominated by the emission line at 622 nm due to $^5D_0 \rightarrow ^7F_2$ intra-4*f* shell transitions with a magnetic final state, the XMCD spectrum measured by XEOL detection uniquely probes the *induced* magnetic moment of the *excited* $^7F_2$ state of Eu³⁺ ions *in the bulk* of the epilayer. The description of the processes underlying the optical detection of XMCD is as follows:

1) X-rays generate Eu³⁺ XEOL by direct excitation following the absorption of an X-ray photon by an atomic level and indirectly through the generation of electron-hole pairs.
2) The $^7F_2$ final state of the $^5D_0 \rightarrow ^7F_2$ transition is populated for ~150 μs after the excitation[19], long enough for the next (probing) X-ray photon to arrive.
3) The X-ray energy is scanned across the Eu $M_{4,5}$ edges and any resulting change in the Eu³⁺ luminescence is monitored.
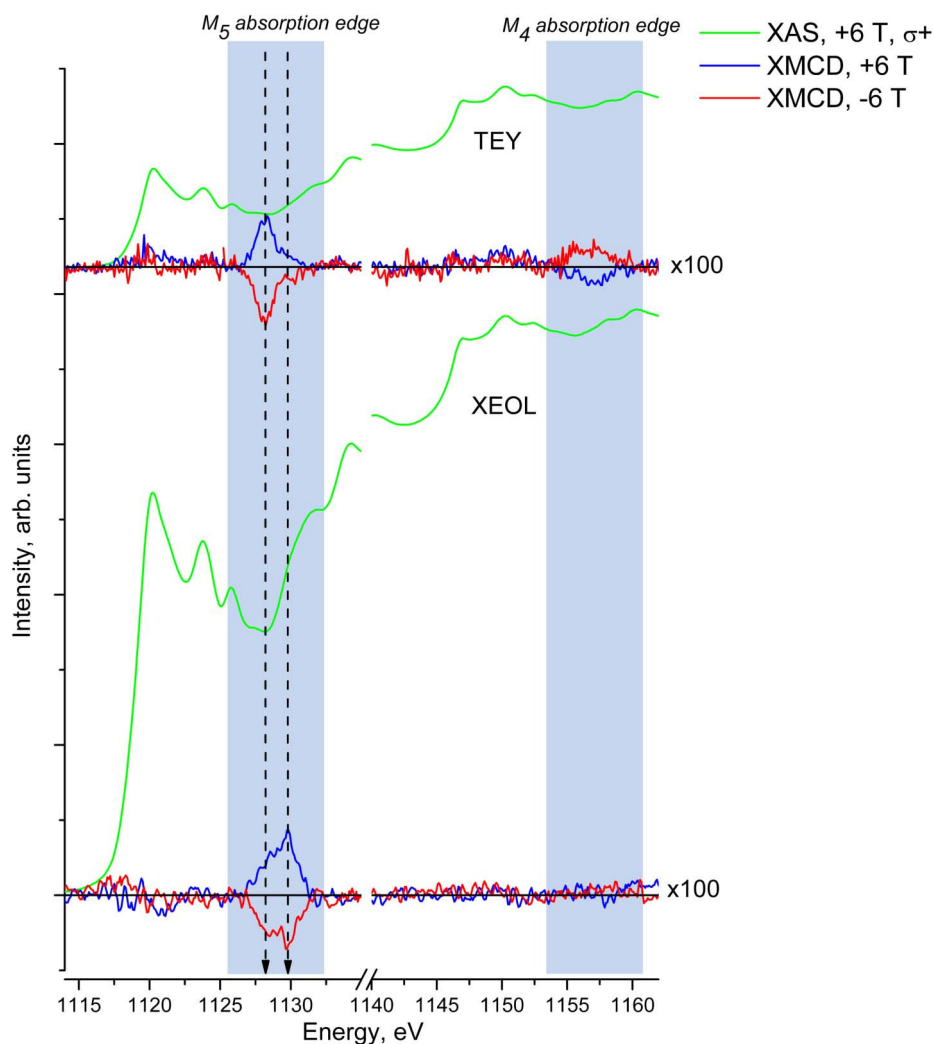
Figure 2 | X-ray absorption and X-ray magnetic circular dichroism. XAS and XMCD spectra measured by detecting the total electron yield and X-ray excited optical luminescence at T = 1.5 K. The vertical dashed lines with arrows indicate the shift of the XMCD peak in TEY and XEOL. The XAS is dominated by the Ga $L_{2,3}$ absorption edges. Spectra are offset vertically for clarity.

Note that in our experiment the X-ray beam is used both as a pump and as a probe. Interestingly, XEOL detection of X-ray absorption spectra was used successfully by Sham *et al.*[21] to explore the origin of luminescence in porous silicon.

The absence of an XMCD signal in XRF can be explained by the fact that the X-ray photon flux incident on the sample ($\sim10^{12}$ photons per second) may not be sufficient to populate the $^7F_2$ states to an adequate detection level, or by the fact that not all Eu^{3+} ions are involved in the process of light emission[17] whereas all Eu^{3+} ions are expected to emit secondary X-ray fluorescence photons. This is to say that the emission of the visible photons following X-ray absorption is intrinsically a more complex process than the emission of X-ray fluorescence photons. Due to the absence of information about the relaxation from higher to lower states of the ^7F_J manifold, however, it is difficult to judge what the primary cause may be.

Atomic multiplet calculations. Theoretical XAS and XMCD spectra for the $M_{4,5}$ absorption of trivalent and divalent Eu ions were calculated using atomic multiplet theory[22]. Spectra for Eu^{2+} $^8S_7$ as well as Eu^{3+} $^7F_0$ and $^7F_2$ are shown in Fig. 3. In the calculation the XMCD peak for $^7F_2$ is shifted by 2.2 eV towards higher energy compared to that for the Eu^{2+} $^8S_7$ state. This energy shift is reproduced very well in the experimentally observed positions of the XEOL and TEY peaks.

X-ray absorption near edge structure. In order to check for the presence of Eu^{2+} in the bulk of the epilayer, the X-ray absorption near edge structure (XANES) of the Eu L_3 absorption edge at 6977 eV[23] was measured using $L\alpha_1$ secondary X-ray fluorescence detection at 5845.7 eV. XANES is a sensitive tool for the determination of the valence states of a particular element in a sample by analyzing the shape and position of the resonance peak, or so called white line[24-27]. In the case of Eu^{2+} and Eu^{3+} the resonance is due to $2p_{3/2}\rightarrow5d$ electronic transitions. The Eu^{2+} and Eu^{3+} valence states can be easily distinguished by the energy position of their white lines. If both Eu^{2+} and Eu^{3+} are present, XANES typically displays two peaks with the stronger one belonging to the dominant oxidation state. The white line for Eu^{2+} species is 7–8 eV lower in energy than that of the Eu^{3+} species[24-27]. The shift in the white line energy position is primarily due to a lower binding energy of the core electrons in Eu^{2+} through shielding of the nucleus by the additional $4f$ electron. Generally, the tabulated value of Eu L_3 X-ray absorption edge energy position of 6977 eV[23] separates the white lines for Eu^{2+} and Eu^{3+} species[24-27]. Fig. 4 shows the analysis of the XANES spectrum for the sample studied. The white line is located at 6980.5 eV with no other peak resolved below 6977 eV. This is a clear indication that no Eu^{2+} is present in the bulk of the epilayer within the sensitivity of XANES measurements. Note that our sample is very dilute with a peak concentration of $\sim9.6\times10^{19}$ cm^{-3} corresponding to an average distance between the Eu^{3+} ions of ~2 nm.
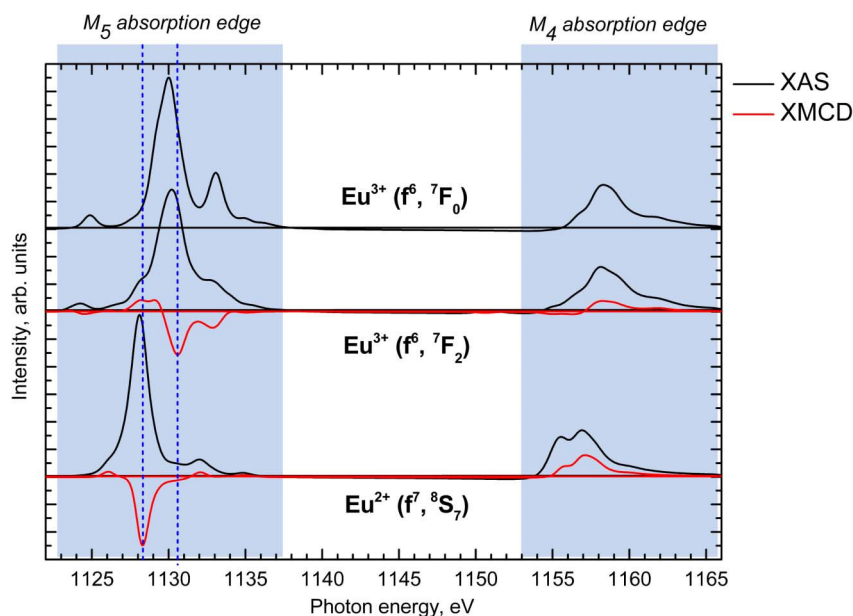
Figure 3 | XAS and XMCD calculated by atomic multiplet theory. Theoretical spectra for Eu $4f^n \rightarrow 3d^9 4f^{n+1}$ transitions. Vertical dashed lines indicate the shift of the calculated M_5 XMCD peaks for Eu^{2+} $^8S_7$ and Eu^{3+} $^7F_2$ states. Spectra are offset vertically for clarity.

Discussion

We report here for the first time the detection of an *induced* magnetic moment of Eu^{3+} ions in the $^7F_2$ state, which is associated with the $^5D_0 \rightarrow {}^7F_2$ intra-4f shell optical emission line at 622 nm. The unique features of Eu^{3+} ions are the non-magnetic $^7F_0$ ground state and magnetic $^7F_{1,2,3}$ states, as displayed in Fig. 1, which can be populated optically or electrically in an LED structure. It is interesting to speculate whether the magnetic moments of the ^7F_J manifold can play a role in the reported room temperature ferromagnetism of Eu-doped GaN. For instance, the $^7F_1$ state is ~70 meV above the $^7F_0$ ground state, so that at room temperature, according to Boltzmann statistics, ~7% of the Eu^{3+} ions will be in the $^7F_1$ state. The sample studied showed ferromagnetic response measured by Superconducting Quantum Interference Device (SQUID) magnetometry, however,

the interpretation of this observation and its relation to the optically induced magnetic moment is a matter for future investigations. Another unique property of Eu^{3+} is its non-magnetic $^5D_0$ excited state. Apart from inducing a magnetic moment by forcing the Eu^{3+} ion to emit a photon, one can *switch off* the induced magnetic moment by *shining light* with an energy *specific* to the transitions from the ^7F_J manifold to the $^5D_0$ state to which GaN is transparent. This opens up a very interesting prospective for electrical or optical manipulations[28] with the excited-state magnetic moments of Eu^{3+} in GaN, which is not feasible with Gd for example since the magnetic moment of Gd cannot be easily switched off. The well-established processing technology for nitride semiconductors should certainly facilitate potential applications of Eu-doped GaN in novel magneto-optoelectronic devices.

Methods

Organometallic vapor phase epitaxy. The growth procedure is described in Ref. 16. Eu-doped GaN layers were grown on a sapphire substrate by OMVPE in Taiyo Nippon Sanso SR-2000 system. Trimethylgallium (TMGa) and ammonia (NH_3) were used as precursors. Tris(dipivaroylmethanato)europium referred to as $Eu(DPM)_3$ was used as a Eu source. The $Eu(DPM)_3$ source temperature was set at ~135°C, while keeping the dopant line temperature at ~145°C to prevent vapor condensation during transport. The growth process consisted of the following steps. First, a 20 nm thick GaN buffer layer was deposited on (0001) sapphire substrate. Then a 4 μm thick undoped GaN layer was grown followed by the deposition of 400 nm thick Eu-doped GaN layer. The pressure in the reactor was 10 kPa. The TMGa and NH_3 flow rate were fixed at 25.5 μmol/min and 8.1 mmol/min respectively. The III/V ratio flow rate was 320. The growth temperature for the sample was 1000°C. Finally, a 10 nm thick GaN cap layer was grown.

Cathodoluminescence spectroscopy. Experiments were carried out using a modified Cameca SX100 electron probe micro-analyser (EPMA). A built-in optical microscope, coaxial and confocal with the electron beam, allows optical monitoring of the sample during measurements. Oriel 0.125 m spectrograph with changeable gratings and a cooled silicon 1024×256 CCD array were inserted in the light path of the optical microscope in order to acquire room temperature CL spectra. A 400 lines/mm diffraction grating was used in the spectrograph. The overall spectral resolution of the system was 0.5 nm.

Figure 4 | X-ray absorption near edge spectroscopy. XANES spectrum was taken at room temperature. Vertical red dashed line indicates the position of the Eu L_3 absorption edge at 6977 eV. Blue short-dashed lines show fitting with a combination of Lorentzian and arctangent functions, which simulate the resonance peak and absorption edge step, respectively. Energy positions of Lorentzian peaks are 6980.5 eV and 6986.5 eV.

X-ray magnetic dichroism measurements. XMCD spectra were measured on beamline I06 at Diamond Light Source, UK. Circularly polarized X-rays were produced by an APPLE II undulator operating in third harmonic. Polarization rate was close to 80%. The beamline operated at its highest possible X-ray photon flux of 10^{12} photons/sec into a spot size of 200 μm (horizontal) by 20 μm (vertical). XMCD spectra were recorded at 1.5 K in a 6 T superconducting magnet using total electron yield and X-ray fluorescence yield detection. X-ray excited optical luminescence was
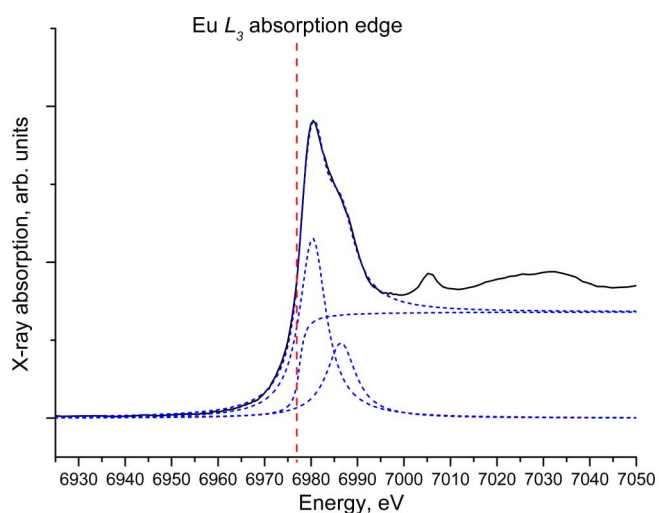
recorded using a Si diode outside the ultrahigh vacuum of the magnet system through a quartz window.

X-ray absorption near edge structure measurements. XANES measurements of Eu L_3 edge were performed on beamline B18 at Diamond Light Source. X-rays produced by a bending magnet were collimated by a Pt-coated collimating mirror and tuned to the desired energy by a Si(111) double crystal monochromator. The X-ray beam was focused to a spot size of 500 μm (horizontal) by 300 μm (vertical) using a Pt-coated double-bend focusing mirror. A pair of Pt coated harmonic rejection mirrors were used for harmonic rejection. Eu $L\alpha_1$ X-ray fluorescence line at 5845.7 eV was detected by a 9-element monolithic Ge detector with XSPRESS-II readout electronics. The Si(111) monochromator was calibrated using the Cr K-edge at 5989 eV prior to the measurements. XANES measurements were done at room temperature. XANES spectra were analyzed by fitting with a combination of Lorentzian and arctangent functions, which simulate the resonance peak and the absorption edge step, respectively.

Atomic multiplet theory. The wave functions of the initial- and final-state configurations for the excitation $4f^n \rightarrow 3d^9 4f^{n+1}$ were calculated in intermediate coupling using Cowan's atomic Hartree-Fock (HF) code with relativistic correction[22,29]. The HF values of the Slater parameters were reduced to 80% to account for screening effects, as was previously found to be the optimal value for the rare-earths $M_{4,5}$ X-ray absorption spectra. Since such an 80% scaling has become standard for rare earths[30], there are essentially no free parameters in the calculation[22].

1. O'Donnell, K. P. & Dierolf, V. (Eds.) *Rare-earth doped III-nitrides for optoelectronic and spintronic applications* (Spinger, Dordrecht, 2010).
2. Kenyon, A. J. Recent developments in rare-earth doped materials for optoelectronics. *Prog. Quantum Electron.* **26**, 225–284 (2002).
3. Henderson, B. & Imbusch, G. F. *Optical spectroscopy of inorganic solids* (Clarendon Press, Oxford, 1989; in Paperback 2006).
4. Favennec, P. N., Haridon, H. L., Salvi, M., Muotonnet, D. & Le Guillo, Y. Luminescence of erbium implanted in various semiconductors: IV, III–V and II–VI materials. *Electron. Lett.* **25**, 718–719 (1989).
5. Dhar, S., Brandt, O., Ramsteiner, M., Sapega, V. F. & Ploog, K. H. Colossal magnetic moment of Gd in GaN. *Phys. Rev. Lett.* **94**, 037205–1/4 (2005).
6. Ney, A., Kammermeier, T., Ollefs, K., Ney, V., Ye, S., Dhar, S., Ploog, K. H., Röver, M., Malindretos, J., Rizzi, A., Wilhelm, F. & Rogalev, A. Gd-doped GaN studied with element specificity: Very small polarization of Ga, paramagnetism of Gd and the formation of magnetic clusters. *J. Magn. Magn. Mater.* **322**, 1162–1166 (2010).
7. O'Donnell, K. P. & Hourahine, B. Rare earth doped III-nitrides for optoelectronics. *Eur. Phys. J.: Appl. Phys.* **36**, 91–103 (2006).
8. O'Donnell, K. P., Martin, R. W. & Middleton, P. G. Origin of luminescence from InGaN diodes. *Phys. Rev. Lett.* **82**, 237–240 (1999).
9. Heikenfeld, J., Garter, M., Lee, D. S., Birkhahn, R. & Steckl, A. J. Red light emission by photoluminescence and electroluminescence from Eu-doped GaN. *Appl. Phys. Lett.* **75**, 1189–1191 (1999).
10. Nishikawa, A., Kawasaki, T., Furukawa, N., Terai, Y. & Fujiwara, Y. Room-temperature red emission from a p-type/europium-doped/n-type gallium nitride light-emitting diode under current injection. *Appl. Phys. Express* **2**, 071004–1/3 (2009).
11. Park, J. H. & Steckl, A. J. Demonstration of a visible laser on silicon using Eu-doped GaN thin films. *J. Appl. Phys.* **98**, 056108–1/3 (2005).
12. Hashimoto, M., Yanase, A., Asano, R., Tanaka, H. & Bang, H. Magnetic properties of Eu-doped GaN grown by molecular beam epitaxy. *Jpn. J. Appl. Phys.* **42**, L1112–L1115 (2003).
13. Hite, J., Thaler, G. T., Khanna, R., Abernathy, C. R., Pearton, S. J., Park, J. H., Steckl, A. J. & Zavada, J. M. Optical and magnetic properties of Eu-doped GaN. *Appl. Phys. Lett.* **89**, 132119–1/3 (2006).
14. Kachkanov, V., O'Donnell, K. P., Rice, C., Wolverson, D., Martin, R. W., Lorenz, K., Alves, E. & Bockowski, M. Zeeman splittings of the $^5D_0$–$^7F_2$ transitions of Eu^{3+} ions implanted into GaN. *Mater. Res. Soc. Proc.* **1290**, mrsf10-1290-i03-06, doi:10.1557/opl.2011.241 (2011).
15. Thole, B. T., van der Laan, G. & Sawatzky, G. A. Strong magnetic dichroism predicted in the M4,5 X-ray absorption spectra of magnetic rare-earth materials. *Phys. Rev. Lett.* **55**, 2086–2088 (1985).
16. Kawasaki, T., Nishikawa, A., Furukawa, N., Terai, Y. & Fujiwara, Y. Effect of growth temperature on Eu-doped GaN layers grown by organometallic vapor phase epitaxy. *Phys. Stat. Sol. (c)* **7**, 2040–2042 (2010).
17. Lorenz, K., Alves, E., Roqan, I. S., O'Donnell, K. P., Nishikawa, A., Fujiwara, Y. & Bockowski, M. Lattice site location of optical centers in GaN:Eu light emitting diode material grown by organometallic vapor phase epitaxy. *Appl. Phys. Lett.* **97**, 111911–1/3 (2010).
18. Dieke, G. H. *Spectra and energy levels of rare-earth ions in crystals* (Interscience Publishers, New York, 1968).
19. Peng, H., Lee, C.-W., Everitt, H. O., Munasinghe, C., Lee, D. S. & Steckl, A. J. Spectroscopic and energy transfer studies of Eu^{3+} centers in GaN. *J. Appl. Phys.* **102**, 073520–1/9 (2007).
20. Maruyama, T., Morishima, S., Bang, H., Akimoto, K. & Nanishi, Y. Valence transition of Eu ions in GaN near the surface. *J. Cryst. Growth* **237–239**, 1167–1171 (2002).
21. Sham, T. K., Jiang, D. T., Coulthard, I., Lorimer, J. W., Feng, X. H., Tan, K. H., Frigo, S. P., Rosenberg, R. A., Houghton, D. C. & Bryskiewicz, B. Origin of luminescence from porous silicon deduced by synchrotron-light-induced optical luminescence. *Nature* **363**, 331–334 (1993).
22. van der Laan, G. Hitchhiker's guide to multiplet calculations. *Lect. Notes Phys.* **697**, 143–199 (2006).
23. Bearden, J. A. & Burr, A. F. Reevaluation of X-ray atomic energy levels. *Rev. Mod. Phys.* **39**, 125–142 (1967).
24. Takanashi, Y., Kolonin, G. R., Shironosova, G. P., Kupriyanova, I. I., Uruga, T. & Shimuzu, H. Determination of the Eu(II)/Eu(III) ratios in minerals by X-ray absorption near-edge structure (XANES) and its application to hydrothermal deposits. *Mineral. Mag.* **69**, 179–190 (2005).
25. Krishnamurthy, V. V., Keavney, D. J., Haskel, D., Lang, J. C., Srajer, G., Sales, B. C., Mandrus, D. G. & Robertson, J. L. Temperature dependence of Eu 4f and Eu 5d magnetizations in the filled skutterudite EuFe$_4$Sb$_{12}$. *Phys. Rev. B* **79**, 014426–1/8 (2009).
26. Korthout, K., Van den Eeckhout, K., Botterman, J., Nikitenko, S., Poelman, D. & Smet, P. F. Luminescence and X-ray absorption measurements of persistent SrAl$_2$O$_4$:Eu,Dy powders: Evidence for valence state changes. *Phys. Rev. B* **84**, 085140–1/7 (2011).
27. Ruck, B. J., Trodahl, H. J., Richter, J. H., Cezar, J. C., Wilhelm, F., Rogalev, A., Antonov, V. N., Binh Do Le. & Meyer, C. Magnetic state of EuN: X-ray magnetic circular dichroism at the Eu $M_{4,5}$ and $L_{2,3}$ absorption edges. *Phys. Rev. B* **83**, 174404–1/6 (2011).
28. Fleischman, Z., Munasinghe, C., Steckl, A. J., Wakahara, A., Zavada, J. & Dierolf, V. Excitation pathways and efficiency of Eu ions in GaN by site-selective spectroscopy. *Appl. Phys. B* **97**, 607–618 (2009).
29. Cowan, R. D. *The theory of atomic structure and spectra* (University of California Press, Berkeley, California, 1981).
30. Thole, B. T., van der Laan, G., Fuggle, J. C., Sawatzky, G. A., Karnatak, R. C. & Esteva, J. M. 3d X-ray-absorption lines and the $3d^9 4f^{n+1}$ multiplets of the lanthanides. *Phys. Rev. B* **32**, 5107–5118 (1985).

Acknowledgements

Author contributions

Y.F. grew the sample. K.P.O'D. and M.J.W. carried out CL measurements. V.K., M.J.W., K.P.O'D, S.S.D., G.v.d.L., S.A.C. carried out XMCD experiments. G.v.d.L. calculated theoretical XAS and XMCD spectra. V.K. and K.P.O'D. carried out XANES measurements. V.K. wrote the paper. All authors commented on the manuscript.

Additional information

How to cite this article: Kachkanov, V. *et al*. Induced magnetic moment of Eu^{3+} ions in GaN. *Sci. Rep.* **2**, 969; DOI:10.1038/srep00969 (2012).